

CHANDRA LETGS SPECTROSCOPY OF IONIZED ABSORBERS: THE QUASAR MR 2251–178

J. M. Ramírez,¹ Stefanie Komossa,¹ Vadim Burwitz,¹ and Smita Mathur²

RESUMEN

Analizamos la observación de MR 2251–178, tomada con el LETGS que se encuentra a bordo de *Chandra*. El absorbedor tibio de MR 2251–178 se puede describir bien con una densidad de columna de $\approx 2 \times 10^{21} \text{ cm}^{-2}$, un parámetro de ionización $\log(\xi) \approx 0.6$, y una velocidad promedio global de $\approx -1100 \text{ km s}^{-1}$. Encontramos en el espectro evidencias de líneas de absorción estrechas producidas por transiciones K_α y K_β de iones de C VI y N VI, que muestran velocidades de eyección (de al menos tres sistemas) ≈ -600 , -2000 y -3000 km s^{-1} . Medimos un flujo en (0.1–2) keV igual a $2.58^{+0.03}_{-0.04} \times 10^{-11} \text{ ergs cm}^{-2} \text{ s}^{-1}$, y un flujo en (2–10) keV de $1.64^{+0.05}_{-0.05} \times 10^{-11} \text{ ergs cm}^{-2} \text{ s}^{-1}$. Esta última medida implica que la fuente nuclear de MR 2251–178 se encuentra en un estado de actividad relativamente bajo. No encontramos evidencias de una componente adicional de absorción que sería generada por una gigantesca región de emisión de [O III], que se encuentra alrededor del núcleo de MR 2251–178. De estar presente, se puede fijar un límite superior en la densidad de columna de $\approx 1.2 \times 10^{20} \text{ cm}^{-2}$. El espectro de rayos X no parece mostrar evidencia fuerte de material polvoso, a pesar de poder establecer límites superiores en las densidades de columnas de carbón y oxígeno neutro en $N_{\text{C I}} \approx 2 \times 10^{19} \text{ cm}^{-2}$ y $N_{\text{O I}} \approx 9 \times 10^{19} \text{ cm}^{-2}$, respectivamente.

ABSTRACT

We analyze the *Chandra* Low Energy Transmission Grating Spectrometer (LETGS) observation of the quasar MR 2251–178. The warm absorber of MR 2251–178 is well described by a hydrogen column density of $\approx 2 \times 10^{21} \text{ cm}^{-2}$, an ionization parameter $\log(\xi) \approx 0.6$, and a global best-fit outflow velocity of $\approx -1100 \text{ km s}^{-1}$. We find in the spectrum evidence of narrow absorption lines. The K_α and K_β transitions of C VI and N VI ions display an outflow with (at least three) components traveling at ≈ -600 , -2000 and -3000 km s^{-1} . We measure a (0.1–2) keV flux of $2.58^{+0.03}_{-0.04} \times 10^{-11} \text{ ergs cm}^{-2} \text{ s}^{-1}$, and a (2–10) keV flux of $1.64^{+0.05}_{-0.05} \times 10^{-11} \text{ ergs cm}^{-2} \text{ s}^{-1}$. This flux implies that the nuclear source of MR 2251–178 is in a relatively low state. We did not find evidence for an extra cold material in the line of sight, that would be associated to the giant [O III] emission region surrounding the nucleus of MR 2251–178. If present, we can set an upper limit of $\approx 1.2 \times 10^{20} \text{ cm}^{-2}$. The X-ray spectrum does not appear to show evidence for dusty material, though an upper limit in the neutral carbon and oxygen column densities can only be set to $N_{\text{C I}} \approx 2 \times 10^{19} \text{ cm}^{-2}$ and $N_{\text{O I}} \approx 9 \times 10^{19} \text{ cm}^{-2}$, respectively.

Key Words: quasars: absorption lines — X-rays: galaxies

1. INTRODUCTION

Warm absorbers (WA) have provided deep insights into the nuclear environment of Active Galaxies (AGN). Halpern (1984) reported its presence for the first time using the *Einstein* observation of the QSO MR 2251–178. Since then, warm absorbers have been commonly found in about 50 % of the AGN spectra (see Komossa & Hasinger 2003, for a review), and their study has enriched our knowledge about the ionization and the kinematics of the gas

composing these systems, important for the understanding of the evolution of these objects, and the AGN unification picture.

Gibson et al. (2005) analyzed data from the *High Energy Transmission Grating* on board *Chandra*, and found evidence in the spectrum of MR 2251–178 of highly ionized, high-velocity ($\sim 12,000 - 17,000 \text{ km s}^{-1}$) outflowing material. They report similar column densities to those of Kaspi et al. (2004), of a few 10^{21} cm^{-2} , and establish conditions for the accretion and mass-loss rates. From the Fe XXVI L_α line, Gibson et al. concluded that, unless the absorber covering factor is very low, the mass-loss rate is approximately an order of magni-

¹Max-Planck-Institut für extraterrestrische Physik, D-85741 Garching, Germany (jramirez@mpe.mpg.de).

²Department of Astronomy, Ohio State University, 140 West 18th Avenue, Columbus, OH 43204, USA.

tude higher than the accretion rate that would provide the radiation power of MR 2251–178 ($\sim 0.2 M_{\odot} \text{ yr}^{-1}$, at 10 % efficiency).

Dusty warm absorbers have been found in a number of AGN Komossa & Hasinger (2003) and are predicted to leave their mark on the X-ray spectra of AGN, for instances the K-edges of O I and C I (Komossa & Fink 1997; Komossa & Bade 1998), and the Fe-L edge, Lee et al. (2001).

For the first time, we search for the presence of a dusty warm absorber in MR 2251–178. Based on ROSAT data, Komossa (2001) speculated about the presence of a second dusty warm absorber in MR 2251–178, but the data did not allow multi-component fitting, which would provide important implications on the global structure of MR 2251–178.

We present an overview and an analysis of the spectrum of MR 2251–178 which we took with the *Low Energy Transmission Grating Spectrometer* (LETGS) on board *Chandra*, (Ramírez et al. 2008). The spectral resolution power of the instrument allows us to confirm some of the previous conclusions about the ionization and the kinematics of the warm absorber of MR 2251–178, and shed new light on the evolution, ionization and composition of this system.

2. GLOBAL SPECTRAL MODELS

2.1. Flux and Luminosity

We integrate an unabsorbed power-law to obtain a flux in the 2 – 10 keV band of $1.64^{+0.05}_{-0.05} \times 10^{-11} \text{ ergs cm}^{-2} \text{ s}^{-1}$, and a (2 – 10) keV source luminosity of $1.62 \times 10^{44} \text{ ergs}^{-1}$. This is $\sim 30\%$ lower than the 2 – 10 keV luminosity measured with the HETGS of $2.41 \times 10^{44} \text{ ergs}^{-1}$. The (0.1 – 2) keV flux is $2.58^{+0.04}_{-0.03} \times 10^{-11} \text{ ergs cm}^{-2} \text{ s}^{-1}$, and the (0.1 – 2) keV luminosity is $2.54 \times 10^{44} \text{ ergs}^{-1}$, a factor of ≈ 1.5 fainter than the ROSAT soft X-ray observation. The information contained from 0.1 – 0.5 keV is important to conclude that the soft X-ray flux is between $\sim 10 - 80\%$ of the hard fluxes historically measured from the spectrum of MR 2251–178.

2.2. Spectral Models

We apply several spectral models to the data, and discuss each in turn. All the models considered in this study are multiplied by an absorption column of gas (phabs model in XSPEC³). The abundances are solar from Anders & Grevesse (1989) with $N_H = 2.77 \times 10^{20} \text{ cm}^{-2}$ to describe the Galactic absorption toward MR 2251–178 (Lockman & Savage

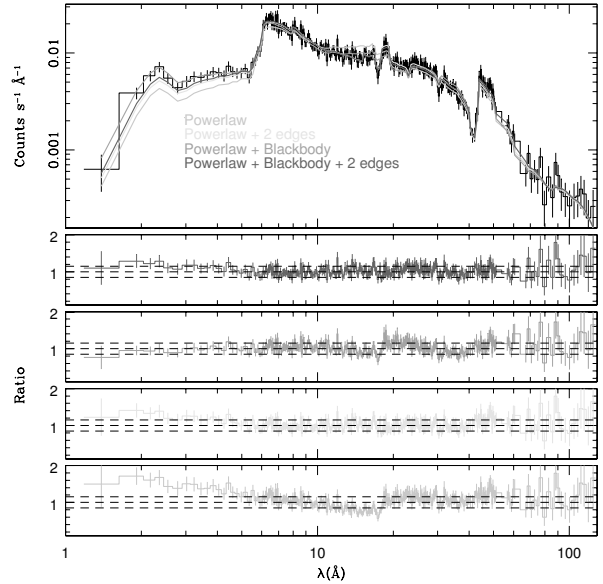


Fig. 1. LETGS spectrum of MR 2251–178 in the observed frame (positive and negative orders added). It is binned to have at least 100 counts from the source per bin. All the models are corrected by the Galactic absorption toward MR 2251–178 (see text). Top panel: Solid lines: p1 (grey), p1 \times 2 edges (lightgrey), p1+bb (mediumgrey), (p1+bb) \times 2 edges (darkgrey). The rest of the panels are the ratios of each composite model to the data, represented by their corresponding grey-scale. (p1=power-law; bb=blackbody).

1995). First, we focus our attention on the fit of a power-law to describe the 1.24–124 Å band of the spectrum. A single power-law gives $\Gamma_x = 1.94^{+0.02}_{-0.02}$, with large residuals (i.e., 15–40 %) in the $\sim 1.2-7$ Å and close to 18 Å (see Figure 1), and a poor statistical fit quality of $\chi^2_{\nu} = 3.00$. We included a thermal component to account for any soft X-ray excess. A blackbody with a temperature of $81.5^{+2.0}_{-2.0}$ eV significantly improved the fit with $\chi^2_{\nu} = 1.63$ (for d.o.f = 305). With this addition, the slope of the power-law changes to a flatter value of $1.53^{+0.02}_{-0.02}$, and the model agrees with the data within 30 % almost from ~ 1.2 to 40 Å, except for the residual around 18 Å.

Now, let us consider the absorption features at ~ 18 Å and ~ 15 Å, in turn. Komossa (2001) fitted a power-law with two edges at the theoretical positions of O VII and O VIII, 739 eV and 871 eV respectively, representing the warm absorber, obtaining $\tau_{\text{O VII}} = 0.22 \pm 0.11$ and $\tau_{\text{O VIII}} = 0.24 \pm 0.12$. Our p1 \times 2 edges (~ 18 Å and ~ 15 Å in the observed frame) model gives us a significant improvement ($\chi^2_{\nu} = 1.38$ for 305 d.o.f) over the fit of the power-law alone

³<http://heasarc.nasa.gov/docs/xanadu/xspec/manual>

($\chi^2_\nu = 3.00$ for 307 d.o.f) and the power-law plus the blackbody component as well ($\chi^2_\nu = 1.63$ for 305 d.o.f). This model is in agreement with the data $\approx \pm 20\%$ (data/model $\approx 1.00 \pm 0.20$) over almost the entire spectrum, except for the wavelength range 1.2–6 Å (and possibly at wavelengths $\gtrsim 60$ Å, but errors are larger). The continuum optical depths are $\tau_{\text{O VII}} = 0.56^{+0.05}_{-0.04}$ and $\tau_{\text{O VIII}} = 0.22^{+0.05}_{-0.04}$. The small errors are due to the high signal-to-noise ratio of this data. We compare these values with those obtained from *ROSAT*. In the case of O VIII they appear to agree within the error bars. However, in the case of O VII the optical depth is approximately a factor of 2.5 higher. In this direct comparison model-to-model, the *Chandra* data suggests that the contribution of this feature has changed over the years (\sim fifteen). A low ionization condition would indeed be consistent with the lower *Chandra* flux compared to the *ROSAT* observation.

Finally, we can build a model combining all the ingredients mentioned above leading us to a global view of the spectrum: A power-law plus a soft-thermal component modified by two warm absorber edges. This model is shown in light blue in Figure 1 and the maximum deviation of the ratio data/model is $\pm 20\%$ over almost the entire spectrum, with $\chi^2_\nu = 1.25$ (for 303 d.o.f). The F-test identifies this improvement as significant (F-test probability $\sim 2 \times 10^{-7}$), over the **p1+2 edges** model. The blackbody has a temperature of ~ 50 eV with the slope of the power-law being in agreement with other models of this study ($\sim 1.7 - 2$) and with slopes reported by previous missions (i.e. *ROSAT*), but not with the flatter slope of ~ 1.4 reported recently by Gibson et al. (2005) in the HETGS observation of the same object. We can see that the inclusion of the strong O VII feature displaces the temperature of the blackbody from ~ 80 to 50 eV with respect to the **p1+bb** without edges. The reduced temperature of the **bb** helps to improve the fit in the range ~ 20 to 60 Å, giving an improvement of $\Delta\chi^2 \sim 110$. The four models are plotted in Figure 1 upon the background subtracted count rate spectrum of MR 2251–178 in the wavelength space (re-binned to have at least 100 counts from the source per bin).

2.3. Warm Absorber - Absorption lines

Using XSTAR ionization models we were able to identify several absorption lines, coming from C VI and N VI, product of electric dipole transitions with the form $1s - np$ for C and $1s^2 - 1snp$ for N ions.

Since most warm absorbers are not at rest, in order to identify, we allowed for a range of outflow

velocities, from 0 – 5000 km s^{-1} . We find that not all of the absorption line candidates are at the same outflow velocity, but we preliminary identify 3 velocities systems at ~ -600 km s^{-1} , -2000 km s^{-1} , and $\sim -3,000$ km s^{-1} .

Based on XSTAR photoionization modelling, we find the observation to be consistent with the resulting spectrum of an absorbing material in our line of sight illuminated by an X-ray source with luminosity of $\sim 10^{44-45}$ erg s^{-1} , atom density $\sim 10^8$ cm^{-3} , column density $\approx 2 \times 10^{21}$ cm^{-2} , and ionization parameter of $\log(\xi) \approx 0.6$. We believe that the inclusion of a thermal component was key to reach this result, otherwise: (1) the absorption structure around 18 Å is not well reproduced, (2) the ionization state of the gas would be higher, bringing a lot of problems in the identification of the atomic transition lines. The temperature of the blackbody used to represent this thermal component is $kT \approx 80$ eV, falling in the soft X-rays. The location of the absorber is estimated to be $\sim 10^{18}$ cm.

We were able to identify four line candidates (in a band where the LETGS has a good performance) at moderate confidence level (90 % level in all the line parameters). Through the K_α and K_β lines of C VI and N VI we find that the flow displays at least three components traveling at velocities $\sim 600 - 3000$ km s^{-1} . We compute $\dot{M} \sim 0.01 f_{\text{cov}} - 0.1 f_{\text{cov}} M_\odot \text{ yr}^{-1}$ and a kinematic energy of $\sim 10^{40-42}$ erg s^{-1} , using these three kinematics systems. This is a factor of a few lower than the accretion rate of the system.

REFERENCES

- Anders, E., & Grevesse, N. 1989, *Geochim. Cosmochim. Acta*, 53, 197
- Gibson, R. R., Marshall, H. L., Canizares, C. R., & Lee, J. C. 2005, *ApJ*, 627, 83
- Halpern, J. P. 1984, *ApJ*, 281, 90
- Kaspi, S., Netzer, H., Chelouche, D., George, I. M., Nandra, K., & Turner, T. J. 2004, *ApJ*, 611, 68
- Komossa, S. 2001, *A&A*, 367, 801
- Komossa, S. & Bade, N. 1998, *A&A*, 331, L49
- Komossa, S. & Fink, H. 1997, *A&A*, 322, 719
- Komossa, S. & Hasinger, G. 2003, in *XEUS - Studying the Evolution of the Hot Universe*, ed. G. Hasinger, T. Boller, & A. N. Parmar (MPE Rep. 281; Garching: MPE), 285
- Lee, J. C., Ogle, P. M., Canizares, C. R., Marshall, H. L., Schulz, N. S., Morales, R., Fabian, A. C., & Iwasawa, K. 2001, *ApJ*, 554, L13
- Lockman, F. J. & Savage, B. D. 1995, *ApJS*, 97, 1
- Ramírez, J. M., Komossa, S., Burwitz, V., & Mathur, S. 2008, *ApJ*, in press (arXiv:0803.3932)